FINITE-DIFFERENCE VECTOR POTENTIAL TIME-DOMAIN APPROACH TO THE ANALYSIS OF PLANAR STRUCTURES

Natalia Georgieva and Eikichi Yamashita
University of Electro-Communications
1-5-1 Chofugaoka, Chofu-shi, Tokyo 182, Japan

ABSTRACT

A time-domain finite-difference approach based on the expression of the field vectors by the vector potential functions is proposed for the analysis of planar structures. The algorithm is theoretically equivalent to the time-domain integral equations (TDIE) approach but is much faster because the calculation of the vector potentials is carried out by the finite-difference wave equation instead of integration. Still integration can be involved when electrically remote objects are present. Only four tangential to the planar interfaces components of the vector potentials are calculated which makes this algorithm advantegous to the FDTD one in respect with storage requirements.

I. INTRODUCTION

Time-domain integral equation (TDIE) approaches were intensively studied and applied to a variety of transient (mainly scattering) problems until Finite-Difference Time-Domain (FDTD) approach was established as a far more efficient and universal way to treat transient fields. TDIE imposed high requirements in respect with CPU time. Besides, they displayed certain problems concerning stability, especially when it comes to electrically thin scatterers ([1],[2]) where the magnetic-field integral equation is entirely unsuitable and the elctric-field integral equation poses numerical problems which is typical for a Fredholm equation of the first kind. Still TDIE have certain advantages - they reduce a 3-D problem to a 2-D one and present a natural way of solving radiation conditions. Recently publications appeared which show successful attempts to combine the advantages of finite-difference techniques with the integral-equation approach [3],[4],[5],[12].

This paper presents a numerical algorithm which combines the advantages of finite-difference schemes with the TDIE approach when applied to planar structures. The approach is a boundary-value one and is based on the surface MFIE and EFIE expressed in terms of vector potentials (VP). At every surface point only four tangential field components are calculated to give the values of the equivalent surface currents exciting the respective four tangential VP components. The VPs are calculated either by direct integration or by the finite-difference wave equation. Both approaches can be combined according to the geometry of the structure. The second approach is much faster and requires the storage of only four VP components' values at every space point but needs a radiation boundary condition when open structures are involved. A numerical absorbing region has been developed to calculate exactly the boundary values of the 3-D numerical domain of the wave equation.

The consistency of the method has been proved by simulations of Gaussian pulse propagation in a homogeneous and an open-end microstrip line. The frequency dependent reflection coefficient of the open-end discontinuity has been calculated. A scattering from a square thin-plate has been also simulated for a Gaussian-pulse incident wave.

II. BASIC EQUATIONS

1. Time-domain vector-potential equations.

From Maxwell equations it follows that the field vectors $\vec{E}$ and $\vec{H}$ can be represented by the magnetic VP $\vec{A}$, the electric VP $\vec{F}$ and the respective scalar potential functions, φ and ψ, as:

$$\vec{E} = -\frac{\partial \vec{A}}{\partial t} - \nabla\varphi - \frac{1}{\varepsilon}\nabla \times \vec{F}, \tag{1}$$

$$\vec{H} = -\frac{\partial \vec{F}}{\partial t} - \nabla\psi + \frac{1}{\mu}\nabla \times \vec{A}. \tag{2}$$

When both magnetic and electric currents,$\vec{K}$ and $\vec{J}$, are present, $\vec{F}$ and $\vec{A}$ satisfy the two inhomogeneous wave equations:

$$\triangle\vec{F} - \frac{1}{v^2}\frac{\partial^2 \vec{F}}{\partial t^2} = -\varepsilon\vec{K} \tag{3}$$

$$\triangle\vec{A} - \frac{1}{v^2}\frac{\partial^2 \vec{A}}{\partial t^2} = -\mu\vec{J}, \tag{4}$$

if the scalar potential functions are related to the VP functions by the Lorentz gauge condition:

$$\frac{\partial \psi}{\partial t} = -v^2\nabla.\vec{F} \tag{5}$$

$$\frac{\partial \varphi}{\partial t} = -v^2\nabla.\vec{A}. \tag{6}$$

Here v is the velocity of light. The free-space solutions of the wave equations for the VP when both surface and volume currents are present are:

$$\vec{F}_{(P,t)} = \frac{\varepsilon}{4\pi}\left[\int_v \frac{\vec{K}(Q,\tau)}{R}dv_Q + \int_s \frac{\vec{K}_s(Q,\tau)}{R}ds_Q\right] \tag{7}$$

0-7803-4603-6/97/$5.00 (c) IEEE

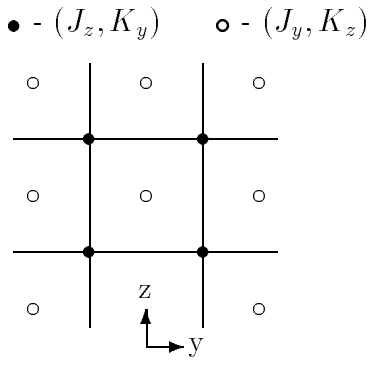

Figure 1: Space displacement of surface currents.

$$\vec{A}_{(P,t)} = \frac{\mu}{4\pi}\left[\int_v \frac{\vec{J}(Q,\tau)}{R}dv_Q + \int_s \frac{\vec{J}(Q,\tau)}{R}ds_Q\right], \qquad (8)$$

where:
R is the distance between the observation point P and the integration point Q;
$\tau = t - R/v$ is the retarded time.
The above equations,when substituted in (1, 2), can be conveniently applied to the solution of boundary - value problems when the equivalence principle is applied. According to the equivalence principle, the region of interest is confined within a surface, the outer fields being assumed equal to zero. Their impact on the internal field is replaced by equivalent sources (surface currents) which satisfy the conditions:

$$\hat{n} \times \vec{H} = \vec{J}_s \qquad (9)$$
$$\hat{n} \times \vec{E} = -\vec{K}_s \qquad (10)$$

where:
$\hat{n}$ is the inward normal of the boundary surface;
$\vec{H}$,$\vec{E}$ are the field vectors at the boundary.
The equivalent sources' contribution is as if they radiate in free space with the dielectric permittivity ε_i and magnetic permeability μ_i of the region of interest (i). Thus, the time-domain boundary integral equation for the tangential field components at the boundary (which are now expressed as equivalent currents) can be obtained. The singularity of the VP functions at surface currents' planes must be considered because the third (curl of the VP) member in equations (1, 2) as expressed with its Cauchy principle value is [6]:

$$\nabla \times \int_s \frac{\vec{J}_s}{R}ds = \oint_s \nabla \times \left[\frac{\vec{J}_s}{R}\right]ds - 2\pi[\hat{n} \times \vec{J}_s].$$

Finally, introducing the incident fields contribution as equivalent currents $\vec{K}^I$ and $\vec{J}^I$, the basic equations for the time-domain VP approach are obtained (the subscript $_s$ for surface currents will be omitted from now on):

$$\vec{K}^{(i)}_{(P,t)} = \frac{1}{2\pi}\hat{n} \times \left[\mu_i \frac{\partial}{\partial t}\oint_s \frac{\vec{J}^{(i)}}{R}ds - \frac{1}{\varepsilon_i}\nabla \int_0^t dt \nabla . \oint_s \frac{\vec{J}^{(i)}}{R}ds + \right.$$
$$\left. + \nabla \times \oint_s \frac{\vec{K}^{(i)}}{R}ds\right] + 2\vec{K}^{I^{(i)}} \qquad (11)$$

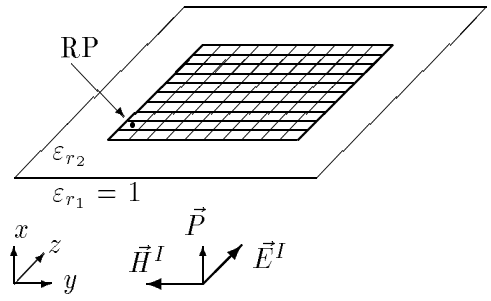

Figure 2: Thin plate scatterer at the air-to-dielectric interface.

$$\vec{J}^{(i)}_{(P,t)} = \frac{1}{2\pi}\hat{n} \times \left[-\varepsilon_i \frac{\partial}{\partial t}\oint_s \frac{\vec{K}^{(i)}}{R}ds + \frac{1}{\mu_i}\nabla \int_0^t dt \nabla . \oint_s \frac{\vec{K}^{(i)}}{R}ds\right.$$
$$\left. + \nabla \times \oint_s \frac{\vec{J}^{(i)}}{R}ds\right] + 2\vec{J}^{I^{(i)}} \qquad (12)$$

Here (i) denotes the respective region. In the above equations it was assumed that there are no volume sources within the region of interest. If there are any, the respective volume integrals should be included. Here all equivalent surface currents in the right-hand side are functions of (Q,τ), where $\tau = t - R/v_i$.

When treating dielectric-to-dielectric interfaces between two regions ($i = 1$ and $i = 2$), equations (11, 12) are coupled by the boundary conditions for their equivalent currents:

$$\vec{K}^{(1)}_s = -\vec{K}^{(2)}_s \qquad (13)$$
$$\vec{J}^{(1)}_s = -\vec{J}^{(2)}_s \qquad (14)$$

In case of a conducting surface $\vec{K}^{(1)}_s = \vec{K}^{(2)}_s = 0$. The equivalent electric currents, $\vec{J}^{(1)}_s$ and $\vec{J}^{(2)}_s$, which are now actual currents, are decoupled. Equations (11) for each region are multiplied by a coefficient α_i $(i = 1, 2)$ and are summed. Similar linear combination is applied to equations (12) with coefficients β_i. The choice of the ratios $\alpha = \alpha_1/\alpha_2$ and $\beta = \beta_1/\beta_2$ is a subject to certain restrictions (see [7],[8],[12]). In this case best results were obtained with $\alpha_1 = \varepsilon_{r_1}$, $\alpha_2 = \varepsilon_{r_2}$, $\beta_1 = \mu_{r_1}$, $\beta_2 = \mu_{r_2}$.

The electric currents at the conducting surfaces of each region (i) are calculated by the magnetic field equation (12).

III. NUMERICAL IMPLEMENTATION

1. Discretization of the numerical space-time domain.

The electric currents and the magnetic currents are displaced in time by a half-step which ensures correct treatment of the time derivatives. For exact evaluation of the space derivatives, $\nabla_s \nabla_s .$ and $\nabla \times$, displacement in space by a half-step is needed, too. The equivalent current components, $(J_z^{k+1/2}, K_y^k)$ and $(J_y^{k+1/2}, K_z^k)$, are located at points displaced by a half-step along both y and z axes (for a plane $x = const$), (Fig.1). The components of $\vec{A}_i$ and $\vec{F}_i$ are calculated at the points of the respective currents.

0-7803-4603-6/97/$5.00 (c) IEEE

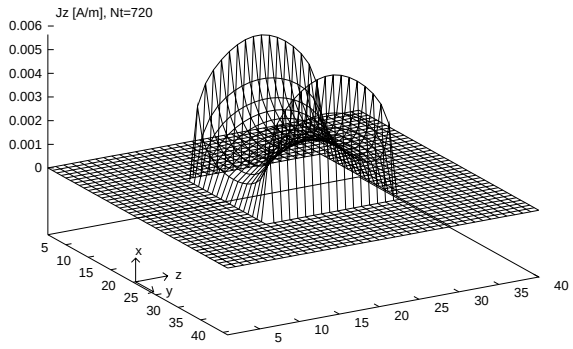

Figure 3: J_z component distribution at the thin plate scatterer, $\varepsilon_{r_2} = 4$,$t = 720\Delta t$.

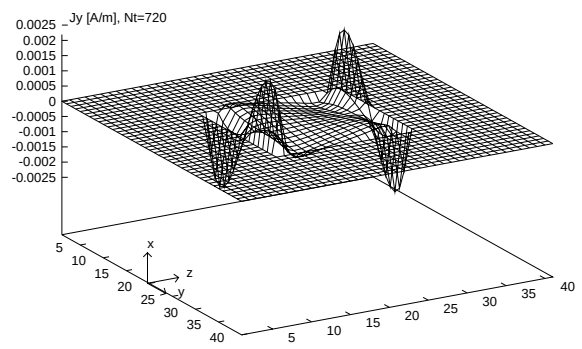

Figure 4: J_y component distribution at the thin plate scatterer, $\varepsilon_{r_2} = 4$,$t = 720\Delta t$.

The time-step Δt and the space-step Δh are related to the higher speed of light in the structure **c** by:

$$\Delta t = \frac{\Delta h}{cq} \tag{15}$$

where q is chosen to be $q = 2$ to ensure stability of the explicit in time finite-difference scheme for the wave equation, [9]:

$$LAP\{f_\xi^k\} - \alpha^2(f_\xi^{k+1} - 2f_\xi^k + f_\xi^{k-1}) = -4\pi g_\xi^k \Delta h \tag{16}$$

where:
$\alpha = q\sqrt{\varepsilon_{r_i}\mu_{r_i}}$;
$LAP = \Delta h^2 \triangle$ is the finite-differenece 3-D Laplacian;
f_ξ is the ξ-component of the VP ($\xi = y, z$);
g_ξ is the surface current component related to the respective VP component.

2. The transmitting boundary for the wave equation.

A field f which propagates in the $+z$ direction satisfies the equation:

$$\frac{\partial f}{\partial z} + \frac{1}{v}\frac{\partial f}{\partial t} = 0, \tag{17}$$

where v is the velocity of propagation in the respective medium. Applying the leap-frog scheme [9] the finite-difference approximation of (17) is obtained:

$$f_{i+1/2}^{k+1/2} = f_{i+1/2}^{k-1/2} - \frac{1}{\alpha^a}(f_{i+1}^k - f_i^k) \tag{18}$$

where $\alpha^a = \Delta h^a/(v\Delta t)$. Here Δh^a is the space-step along the direction of propagation in an additional absorbing buffer region adjacent to the main region of the wave equation. The best performance of this scheme is achieved when $\alpha^a = 1$. Therefore, the discretization step of the main region Δh is greater than Δh^a:

$$\Delta h^a = \frac{\Delta h}{q\sqrt{\varepsilon_r\mu_r}} \tag{19}$$

where ε_r and μ_r are the constants of the relative medium.

IV. RESULTS AND DISCUSSION

Two types of simulations are presented - a scattering problem and a transmission line problem.

1. Scattering of an infinitesimally thin plate.

The scatterer is an infinitesimally thin square plate at the interface between air (region 1) and dielectric (region 2) with dielectric constant ε_{r_2}. Two simulations were carried out - for $\varepsilon_{r_2} = 1$ and $\varepsilon_{r_2} = 4$. The incident wave is a Gaussian pulse in time. The presented results are for the case of normal incidence. The time-response for the J_z component at a given reference point (point RP in Fig.2) is presented to verify the field behaviour in time. The reference point is located three steps along the z-axis and one step along the y-axis from the front-left corner of the plate. The scattering plate's size is A=$16\Delta h$ ($\Delta h = 0.6m$).

A typical space distribution of the surface currents for the case is presented in Fig.3, Fig.4. Fig.5 represents the time-response for the total current component J_z for both $\varepsilon_r = 1$ and $\varepsilon_r = 4$ at the reference point RP. Here the total current has been calculated as:

$$\vec{J} = \vec{J}_1 + \vec{J}_2$$

The resonant character of the time-response is well seen, as well as the influence of the dielectric layer on the resonant frequency of the same patch. The frequency response of the time-data for J_z are presented in Fig.6.

2. Open-end microstrip line.

The dispersive character of the reflection coefficient S_{11} was investigated for the open-end discontinuity in a microstrip line. The dimensions of the structure and the dielectric constant of the substrate were chosen exactly as in [11] to compare the results with those obtained by FDTD method:

dielectric constant: $\varepsilon_r = 9.6$;
strip width: $W = 0.6\ mm$;
substrate thickness: $H = 0.6\ mm$.

Discretization step in space has been chosen $\Delta h = W/8$.
The dimensions of the whole numerical plane are:

length $L = 140\Delta h$;
width $A = 30\Delta h$;
height $B = 3H$.

0-7803-4603-6/97/$5.00 (c)

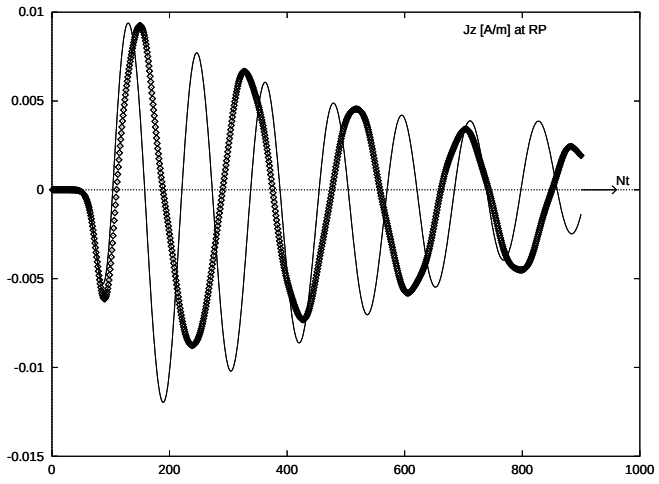

Figure 5: J_z component time-response at reference point RP. With lines - $\varepsilon_{r_2} = 1$; with points - $\varepsilon_{r_2} = 4$.

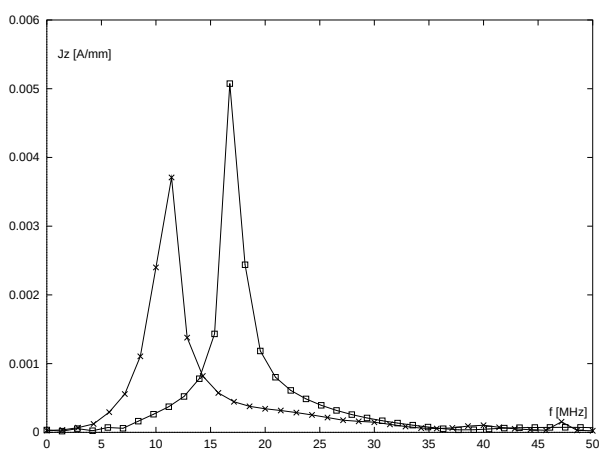

Figure 6: J_z component frequency-response at reference point RP. With boxes - $\varepsilon_{r_2} = 1$; with crosses - $\varepsilon_{r_2} = 4$.

Fig. 7 shows the results for the magnitude of S_{11} which are in good agreement with those given in [11].

CONCLUSION

A new finite-difference time-domain approach for the analysis of planar structures has been developed. It reduces the number of unknown field quantities to four tangential components of the respective vector potentials, thus, reducing memory and CPU time requirements in comparison with FDTD method. The method is equally well-suited for open and closed problems and allows for both integration and finite-difference wave equation calculation of the vector potentials. Further investigations on improving the absorbing boundaries and increasing the overall speed of the numerical algorithm can make it suitable for the analysis of far more complicated than the considered ones planar structures.

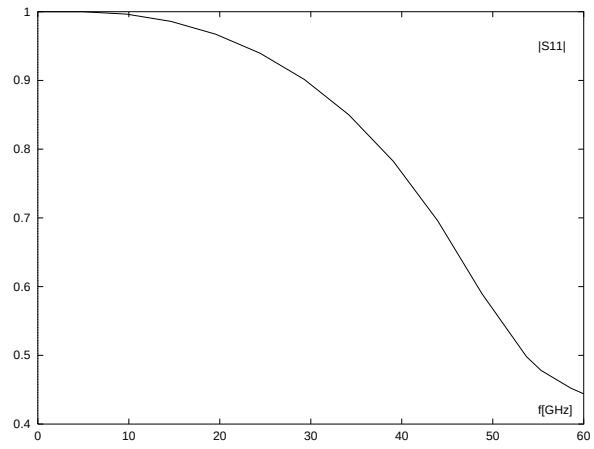

Figure 7: $|S_{11}|$ of the open-end microstrip line.

References

[1] L.B. Felsen ed., *Transient Electromagnetic Fields*, Springer - Verlag, 1976

[2] R. Mittra, Y.Rahmat-Samii, D.V. Jamnejad, W.A. Davis, 'A New Look at the Thin-Plate Scattering Problem', *Radio Science*, Vol. 8, No 10, Oct 1973

[3] D.A. Vechinski and S.M. Rao, T.K. Sarkar, 'Transient Scattering from Three-Dimensional Arbitrarily Shaped Dielectric Bodies', *J Opt. Soc. Am A*, vol. 11, No 4, April 1994

[4] J.M. Johnson, Y. Rahmat-Samii, 'Multiple Region FDTD (MR/FDTD) and its Application to Microwave Analysis and Modeling', *IEEE MTT-S Symposium*, San Francisco, June 1996

[5] N. Georgieva and E. Yamashita, 'Analysis Method for Transient Fields in Planar Structures by Marching-on-in-Time Integral Equation Technique', *IEEE MTT-S Symposium*, San Francisco, June 1996

[6] D. Colton,R. Kress, *Integral Equation Methods in Scattering Theory*, John Wiley & Sons, 1983

[7] J.R. Mautz and R.F. Harrington, 'Electromagnetic Scattering from a Homogeneous Body of Revolution', *Dept. Elect. Comput. Eng., Syracuse Univ., TR-77-10*, November 1977

[8] H. Mieras, C.L. Bennett, 'Space-Time Integral Equation Approach to Dielectric Targets', *IEEE Trans. AP*, vol. AP-30, No 1, Jan. 1982

[9] John C. Strikwerda, *Finite Difference Schemes and Partial Differential Equations*, Wadsworth & Brooks / Cole Mathematics Series, 1989

[10] K.S. Kunz and R.J. Luebbers, *Finite-Difference Time-Domain Method for Electromagnetics*, CRC Press, 1993

[11] X. Zhang and K.K. Mei, 'Time-Domain Finite-Difference Approach to the Calculation of the Frequency-Dependent Characteristics of Microstrip Discontinuities', *IEEE Trans. on MTT*, vol. 36, No 12, December 1988

[12] N. Georgieva and E.Yamashita, 'Finite Difference Approach to the Solution of Time-Domain Integral Equations for Layered Structures', to be published in *IEEE Trans. on MTT*